Coherent Vortex Extraction in 3D Turbulent Flows Using Orthogonal Wavelets

Marie Farge,[1] Giulio Pellegrino,[2] and Kai Schneider[3]

[1]*Laboratoire de Météorologie Dynamique du CNRS, Ecole Normale Supérieure, Paris, France*
[2]*Institut für Chemische Technik, Universität Karlsruhe (TH), Germany*
[3]*Centre de Mathématiques et d'Informatique, Université de Provence, Marseille, France*

This Letter presents a wavelet technique for extracting coherent vortices from three-dimensional turbulent flows, which is applied to a homogeneous isotropic turbulent flow at resolution $N = 256^3$. The coherent flow is reconstructed from only $3\%N$ wavelet coefficients that retain the vortex tubes, and 98.9% of the energy with the same $k^{-5/3}$ spectrum as the total flow. In contrast, the remaining $97\%N$ wavelet coefficients correspond to the incoherent flow which is structureless, decorrelated, and whose effect can therefore be modeled statistically.

In this Letter we propose a wavelet method to split turbulent flows into organized and random components. It follows the prescription given by Hugh Dryden half a century ago when he wrote [1] "The rapidly developing theory of random functions may possibly form the mathematical framework of an improved theory of turbulence. However, it is necessary to separate the random processes from the nonrandom processes. It is not yet fully clear what the random elements are in turbulent flows." We conjecture that turbulent flows can be described as a superposition of metastable coherent vortices that are not in statistical equilibrium. Their nonlinear interactions are responsible for the chaotic behavior of turbulent flows and generate a random incoherent flow, which then relaxes towards statistical equilibrium and is dissipated at the smallest scales. This leads us to define a new method, called coherent vortex simulation (CVS) [2,3], which splits each flow realization into coherent and random contributions and computes the time evolution of only the former, while modeling the effect of the latter.

Such a separation is not possible in the Fourier representation, as turbulent flows have no spectral gap that allows decoupling out-of-equilibrium large-scale motions and well-thermalized small-scale motions. This explains why the concepts which have been derived by analogy with the kinetic theory of gases (e.g., mixing length, turbulent viscosity, homogenization, renormalization, subgrid scale parametrization) have encountered problems in modeling turbulent flows. We conjecture that the wavelet representation, formulated in terms of both space and scale [4,5], allows such a decoupling between organized motions out of statistical equilibrium and random motions in statistical equilibrium. Both components are multiscale [6] but have different probability distributions and correlations.

To perform the CVS decomposition we use vorticity rather than velocity because it is more appropriate for tracking the nonlinear dynamics of turbulent flows, in any space dimension, since vorticity is independent of the inertial frame (Galilean invariance) and has strong topo-

logical properties expressed in Helmholtz' and Kelvin's theorems. Moreover, vorticity compresses better than velocity in a wavelet basis, because it is more localized in space.

The principle of the CVS method, as we have already demonstrated for two-dimensional flows [2], is to split the vorticity field into two orthogonal fields. After projecting the vorticity field onto an orthogonal wavelet basis, the coherent vorticity is reconstructed from the wavelet coefficients larger than a given threshold and the incoherent vorticity from the remaining wavelet coefficients. Finally, the coherent and incoherent velocities are computed from the coherent and incoherent vorticities using Biot-Savart law. The threshold value depends on the variance of the total field, i.e., the total enstrophy, and on its resolution, without any adjustable parameter. This choice is based on theorems [7] proving optimality of the wavelet representation to denoise signals having inhomogeneous regularity, such as the intermittent fields encountered in turbulence. The CVS decomposition gives a constructive definition of the coherent vortices and of the incoherent background flow.

In this Letter we generalize the CVS decomposition to three-dimensional turbulent flows. Each of the three components ω_k of vorticity is projected onto an orthogonal wavelet basis ψ_Λ, constituting a MRA (multiresolution analysis) [4,5], where $\Lambda = (j, \vec{i}, \mu)$ indexes the scale j, the three space coordinates $\vec{i}$, and the seven spatial directions μ. We thus obtain the wavelet coefficients $\tilde{\omega}_i = \langle \omega, \psi_\Lambda \rangle$, where $\langle ., . \rangle$ is the inner product. We then compute the modulus of the vorticity wavelet coefficients $|\tilde{\omega}|$ and determine the index set Λ_C addressing the coherent wavelet coefficients $(\tilde{\omega}_k)_C$ whose absolute value is larger than the threshold $|\tilde{\omega}|_T = (\frac{4}{3}Z \log N)^{1/2}$, where $Z = \frac{1}{2}\langle \omega, \omega \rangle$ is the total enstrophy and N the resolution. The complementary index set $\Lambda_I = \Lambda \backslash \Lambda_C$ addresses the incoherent wavelet coefficients $(\tilde{\omega}_k)_I$. Subsequently, we reconstruct by inverse wavelet transform each component of the coherent and incoherent vorticity fields and obtain the decomposition of the total vorticity into

$\vec{\omega} = \vec{\omega}_C + \vec{\omega}_I$. Note that the wavelet transform is orthogonal, which yields the decomposition of the total enstrophy into $Z = Z_C + Z_I$. Finally, the Biot-Savart law $\vec{V} = \nabla \times (\nabla^{-2}\vec{\omega})$ is used to compute the corresponding coherent and incoherent velocity fields to obtain $\vec{V} = \vec{V}_C + \vec{V}_I$. Moreover, since wavelets are almost eigenfunctions of the Biot-Savart kernel, the total energy is also split into $E = E_C + E_I + \epsilon$ with $E = \frac{1}{2}\langle\vec{V},\vec{V}\rangle$ and $\epsilon \leq 0.5\%E$.

To illustrate CVS filtering, we consider a statistically stationary three-dimensional homogeneous isotropic turbulent flow, forced at large scale, with a microscale Reynolds number $R_\lambda = 150$. The initial conditions are random and the boundary conditions are periodic. This flow was computed by Vincent and Meneguzzi [8] using a pseudospectral code at resolution 240^3, upsampled to $N = 256^3$. Such a fully developed turbulent flow contains organized vortex tubes (also called vortex filaments or "worms"), observed in both numerical [8,9] and laboratory experiments [10], which are advected in a homogeneous and isotropic fashion by the velocity field they generate.

In applying the CVS extraction algorithm with Coifman 12 wavelets [4,5], we find that the coherent flow is represented by only $3\%N$ wavelet coefficients, although it retains 98.9% of the energy and 75.4% of the enstrophy. In contrast, the incoherent flow, which corresponds to the $97\%N$ remaining wavelet coefficients, contains only 0.6% of the energy and 24.6% of the enstrophy. In Fig. 1 we observe that both the coherent and incoherent fields are multiscale, which confirms previous works [2,4,6,8]. The energy spectrum for the coherent flow has the same $k^{-5/3}$ scaling as the total flow, throughout the whole inertial range. The fall off observed in the dissipative range corresponds to some coherent energy which has been transferred into incoherent energy before being dissipated. This is confirmed by the fact that there is an equipartition of incoherent energy up to the dissipative scales, since its spectrum scales as k^2 (white noise in 3D) followed by a decay

due to the dissipation of incoherent energy at the smallest scales.

We now compare the total, coherent, and incoherent vorticity fields in physical space, after zooming into a 64^3 subcube to observe the small scale structures. Figures 2, 3, and 4 show three isosurfaces of the modulus of vorticity $|\vec{\omega}|$ for each of the three fields. We find the same entangled vortex tubes in the coherent vorticity (Fig. 3) as in the total vorticity (Fig. 2), while the incoherent vorticity is structureless (Fig. 4). The decomposition of the turbulent flow into an organized coherent contribution and a random incoherent contribution is confirmed by looking at the PDFs (probability distribution functions) of velocity and vorticity. In Fig. 5 we observe that the coherent velocity has exactly the same PDF as the total velocity, and that the PDF of the incoherent velocity PDF is Gaussian with a variance ten times smaller than that of the total velocity. In Fig. 6 the PDF of the coherent vorticity exhibits the same stretched exponential behavior as the total vorticity, while the PDF of the incoherent vorticity is exponential with a much smaller variance. Note that we have plotted only one component of velocity and of vorticity, since we have checked that, for both fields, the three components have the same PDF.

The CVS extraction algorithm is based on a wavelet denoising method without any *a priori* assumption as to the shape of the coherent vortices. We now check *a posteriori* that the coherent vorticity field indeed contains the vortex tubes observed in fully developed turbulent flows [8–10]. The vortex tubes are local quasisteady solutions of Euler equations, which occur in regions where the nonlinearity is depleted. In 2D turbulent flows these regions
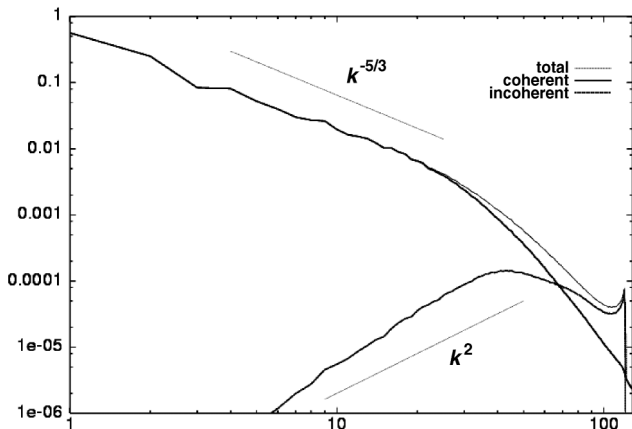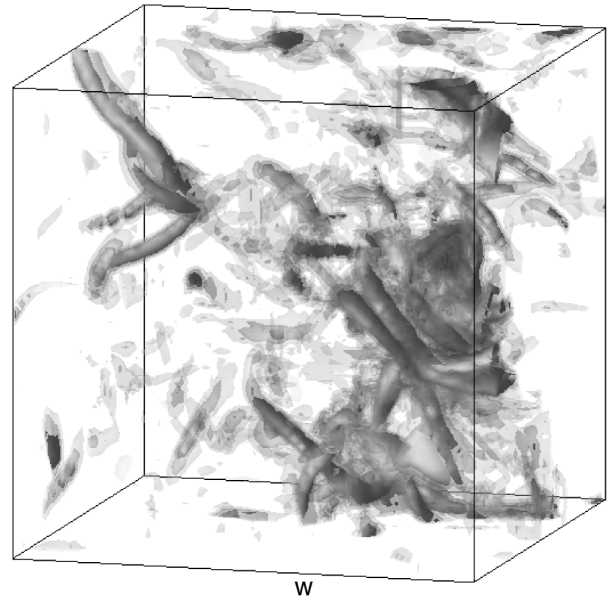

FIG. 1. Energy spectrum $E(k)$.

FIG. 2. Total vorticity (the gray surfaces, from light to dark, correspond to $|\vec{\omega}| = 3\sigma$, 4σ, and 5σ, with $\sigma = \sqrt{2Z}$).
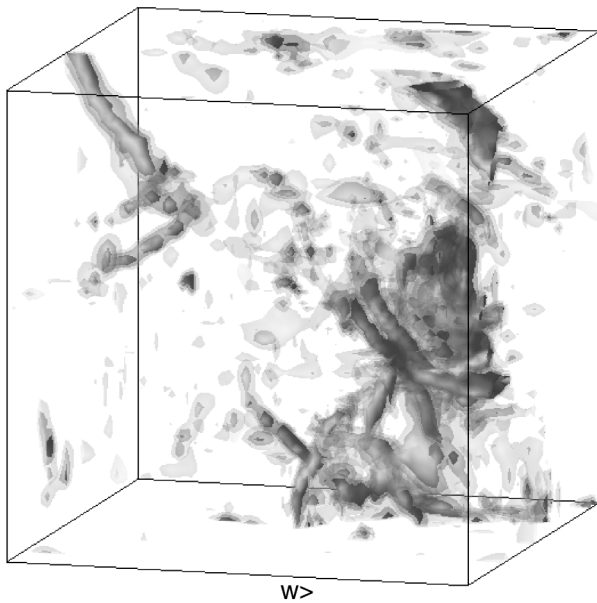
FIG. 3.   Coherent vorticity (the gray surfaces, from light to dark, correspond to $|\vec{\omega}| = 3\sigma, 4\sigma$, and 5σ).

are characterized by a functional relationship between vorticity and stream function which is used to identify the coherent vortices [2]. However, such a precise criterion to characterize them does not yet exist for 3D turbulent flows, since their dynamics is more complicated due to vortex stretching. If we rewrite Euler equations in terms of the Lamb vector $\vec{l} = \vec{V} \times \vec{\omega}$, we obtain $\partial_t\vec{\omega} + \nabla \times \vec{l} = 0$ and $\nabla \cdot \vec{V} = 0$. Thus, one possibility for the nonlinearity to be depleted is when $\vec{V}$ tends to align with $\vec{\omega}$. This corresponds to the local maximization of the relative helicity
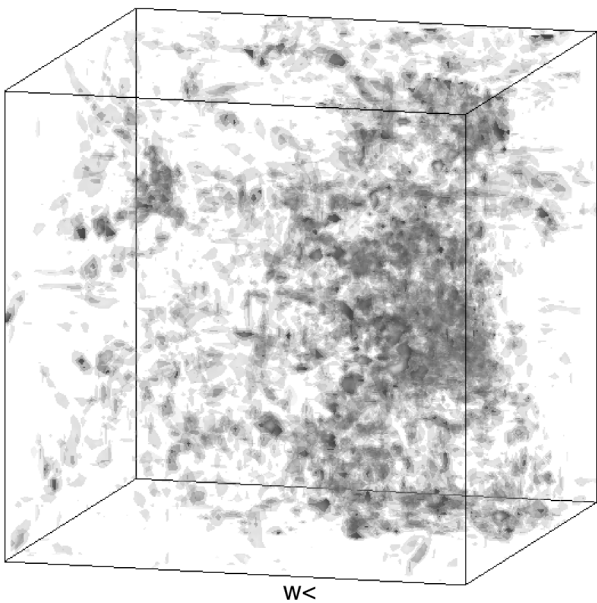

FIG. 4.   Incoherent vorticity (the gray surfaces, from light to dark, correspond to $|\vec{\omega}| = 3/2\sigma, 2\sigma$, and $5/2\sigma$).
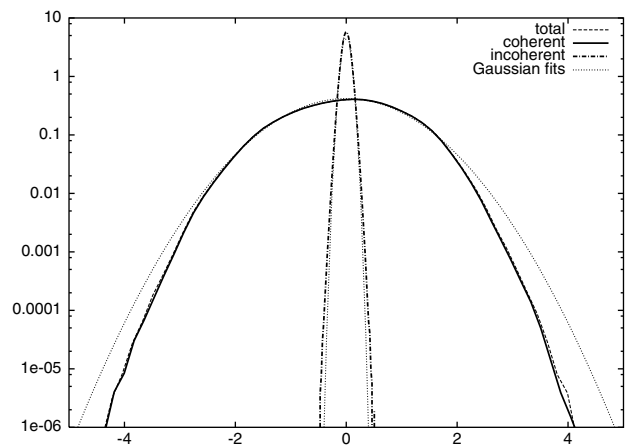

FIG. 5.   PDF of velocity.

$h = \frac{\vec{V}\cdot\vec{\omega}}{|\vec{V}||\vec{\omega}|}$ and is called local Beltramization. Moreover, it has been observed in both laboratory and numerical experiments that vortex tubes maximize helicity [11,12], therefore we will use the relative helicity h as an indication of their presence. In Fig. 7 we plot the PDF of h for the total, coherent, and incoherent flows, and we observe that the coherent flow exhibits the same distribution as the total flow, with two maxima at $h = +1$ and -1 corresponding to alignment and antialignment between $\vec{\omega}$ and $\vec{V}$ (note that two 3D random fields would have a flat PDF of h). The fact that the coherent flow presents the same tendency towards local Beltramization as the total flow is another confirmation that the CVS filtering has extracted the vortex tubes. In contrast, the PDF of h for the incoherent flow is more evenly distributed with a maximum at $h = 0$, which suggests a tendency towards two-dimensionalization. These observations support Moffatt's conjecture that "blobs of maximal helicity may be interpreted as coherent structures, separated by regular surfaces on which vortex sheets, the site of strong dissipation, may be located" [13].

In conclusion, we have shown that the coherent flow contains the vortex tubes and has the same $k^{-5/3}$
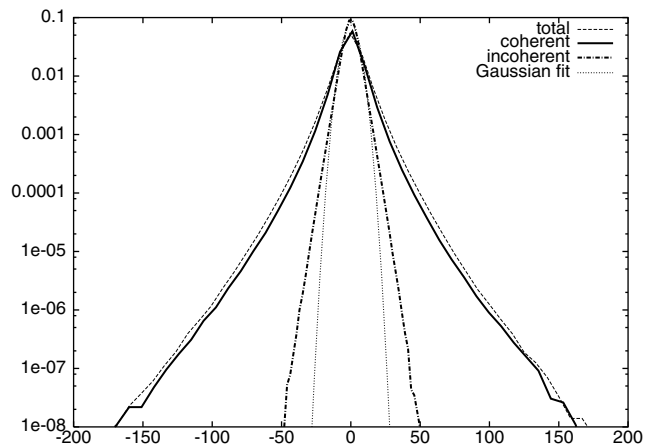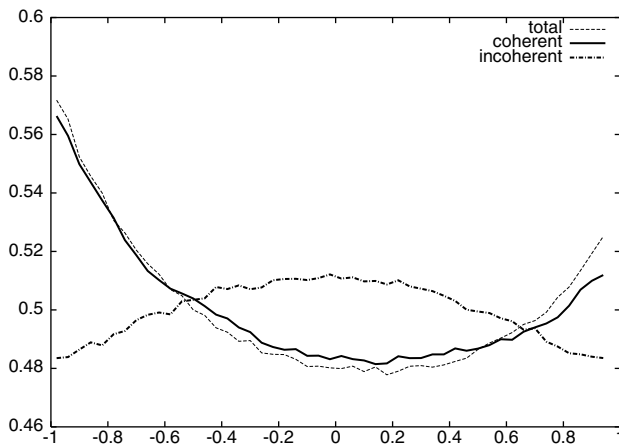

FIG. 6.   PDF of vorticity.

FIG. 7. PDF of relative helicity.

power-law behavior as the total flow. This leads us to propose a new scenario to explain the turbulent cascade. The transfer of energy between the various scales does not result from eddy fragmentation, as in the classical Richardson's scenario. It is rather due to nonlinear vortex interactions, e.g., stretching and straining, which transfer coherent energy throughout the whole inertial range, while at the same time producing incoherent energy, which is present at all inertial scales, and is dissipated only at the smallest scales.

CVS is based on the hypothesis that there is no need to compute the evolution of the incoherent degrees of freedom, since they have reached statistical equilibrium. Evidence for this has been given in this Letter by the following observations: the incoherent flow is structureless, decorrelated (since it presents an equipartition energy spectrum) and its velocity PDF is Gaussian. Thus, the effect of the incoherent degrees of freedom on the coherent ones can be modeled statistically. In contrast, the coherent degrees of freedom are out of statistical equilibrium, since they correspond to long-range correlated vortex tubes in nonlinear interaction. Therefore their evolution should be computed in detail by tracking their displacements and the production of strong gradients.

The results presented in this Letter give us incentives to extend the CVS method to compute three-dimensional Navier-Stokes equations in an adaptive wavelet basis, remapped at each time step to track the nonlinear vortex dynamics in both space and scale, as we have done for two-dimensional turbulent flows [2,3]. The advantage of the CVS method is to combine an Eulerian representation of the solution in a wavelet basis with a Lagrangian strategy to adapt the basis in space and scale, to track the formation, advection, and dissipation of vortex tubes whatever their scales.

[1] H. L. Dryden, Adv. Appl. Mech. **1**, 1 (1948).
[2] M. Farge, K. Schneider, and N. Kevlahan, Phys. Fluids **11**, 2187 (1999).
[3] K. Schneider, N. Kevlahan, and M. Farge, Theor. Comput. Fluid Dyn. **9**, 191 (1997).
[4] M. Farge, Annu. Rev. Fluid Mech. **24**, 395 (1992).
[5] S. Mallat, *A Wavelet Tour of Signal Processing* (Academic Press, New York, 1997).
[6] M. Farge and G. Rabreau, C. R. Acad. Sci. Ser. IIb **307**, 1479 (1988).
[7] D. Donoho, Appl. Comput. Harmon. Anal. **1**, 100 (1993).
[8] A. Vincent and M. Meneguzzi, J. Fluid Mech. **258**, 245 (1994).
[9] E. D. Siggia, J. Fluid Mech. **107**, 375 (1981).
[10] S. Douady, Y. Couder, and M. E. Brachet, Phys. Rev. Lett. **67**, 983 (1991).
[11] E. Levich, Phys. Rep. **151**, 129 (1987).
[12] A. Tsinober and E. Levich, Phys. Lett. **99A**, 321 (1983).
[13] H. K. Moffatt, J. Fluid Mech. **150**, 359 (1985).